

Dynamic Properties of the Feedback Control of a Distributed Delay Logistic Differential Equation

Ahmed M. A. El-Sayed¹, Sanaa M. Salman², Muhammed A. Saad^{1,*}

¹ Mathematics and Computer Science Department, Faculty of Science, Alexandria University, Alexandria, Egypt.

² Mathematics Department, Faculty of Education, Alexandria University, Alexandria, Egypt.

* Correspondence Address:

Muhammed. A. Saad: Mathematics and Computer Science Department, Faculty of Science, Alexandria University, Alexandria, Egypt.
Email address: muhammed.Saad@alexu.edu.eg.

KEYWORDS: Logistic, Distributed, Delay, Bifurcation, Chaos.

Received:

January 21, 2025

Accepted:

February 19, 2025

Published:

May 16, 2025

ABSTRACT: This paper investigates the stability characteristics of the logistic differential equation with distributed delay, exploring its dynamics in both discrete and continuous time frameworks. By examining the influence of varying system parameters, particularly the delay kernel, the study provides a comprehensive understanding of how these factors shape system stability. The analysis employs numerical simulations to delineate stability regions, focusing on the interplay between parameter variations and dynamic behavior. Key findings highlight the critical role of the delay kernel in determining the transition between stable and unstable states. Numerical results are presented through visual tools such as phase portraits and plots of the maximal Lyapunov exponent, which capture the progression from stable equilibrium to oscillatory or chaotic dynamics. These illustrations offer valuable insights into the mechanisms underlying stability loss and the onset of complex behaviors. The study emphasizes the sensitivity of the logistic model to distributed delay variations, showcasing the intricate dependency of system behavior on the kernel's properties. This sensitivity is pivotal in understanding the dynamics of real-world systems modeled by logistic equations with delay. Moreover, the results have broad implications for applications where distributed delay plays a significant role, such as population dynamics, biological systems, and control theory. By elucidating the relationship between delay kernels, parameter changes, and system stability, this work contributes to a deeper understanding of delayed dynamical systems and their practical applications. The findings underscore the importance of delay structure in predicting and controlling system behavior.

1. INTRODUCTION

Logistic differential equations have long been recognized as a cornerstone in mathematical modeling, particularly in the study of population dynamics. The classical logistic model, introduced by Verhulst in the 19th century, captures the essence of growth processes constrained by limited resources. This model assumes that the rate of population growth is proportional to both the current population size and the remaining capacity of the environment. The Logistic

equation [1] is given by:

$$\frac{dx(t)}{dt} = \rho x(t) \left(1 - \frac{x(t)}{k}\right). \quad (1.1)$$

where $x(t)$ represents the population size at time t , ρ is the intrinsic growth rate, and k is the carrying capacity of the environment.

While this model effectively describes simple population dynamics, real-world systems often exhibit complexities that necessitate extensions to the classical formulation.

One such extension involves incorporating time delays, resulting in delay differential equations (DDEs). Time delays arise naturally in many biological, ecological, and physical systems due to factors such as gestation periods, maturation times, and delayed environmental feedback. These delays significantly influence system behavior, introducing phenomena such as oscillations, bifurcations, and chaotic dynamics. Among these, the delay logistic equation stands out as a fundamental tool for capturing population growth processes where current growth rates depend on past states [2].

The delay logistic equation with a fixed delay τ is given by:

$$\frac{dx(t)}{dt} = \rho x(t) \left(1 - \frac{x(t-\tau)}{k}\right). \quad (1.2)$$

where τ is specific lags in reproduction or resource utilization. While this model enhances realism, it is often limited in capturing the broader influence of historical population states over a continuous time range [3].

The multiple delays model accounts for various delays, denoted as τ_i , each associated with a specific coefficient α_i , reflecting distinct lagging processes. This approach is particularly effective in representing ecosystems influenced by multiple factors, where each factor has its own delay attributes. Examples include climatic variations, resource availability, and human interventions, all of which can concurrently impact population dynamics [4].

$$\frac{dx(t)}{dt} = \rho x(t) \left(1 - \frac{1}{k} \sum_{i=1}^n \alpha_i x(t - \tau_i)\right). \quad (1.3)$$

On the other hand, the distributed delay framework offers a more versatile approach for modeling systems where feedback processes are gradual rather than instantaneous. For instance, in ecosystems, factors such as resource regeneration, competition, and environmental changes often exert their influence over an extended period. By incorporating distributed delays, these models provide deeper insights into the stability and dynamic behavior of complex systems.

$$\frac{dx(t)}{dt} = \rho x(t) \left(1 - \frac{1}{k} \int_0^t G(t-s) x(s) ds\right). \quad (1.4)$$

The concept of distributed delays in DDEs extends the idea of a discrete delay by considering a delay that is spread over a range of times rather than occurring at a single fixed point. This approach is especially useful in modeling systems where the influence of past states is distributed over a continuum of past times [5, 6, 7, 8].

The equation can be rewritten by assuming $k = 1$ as follows:

$$\frac{dx(t)}{dt} = \left(\rho x(t) - \rho x(t) \int_0^t G(t-s) x(s) ds\right). \quad (1.5)$$

Recent studies have highlighted the importance of distributed delay models in diverse applications, ranging from ecological systems to epidemiology and economic modeling. For example, Zhang et al. explored the impact of distributed delays on predator-prey systems, revealing how such delays can stabilize or destabilize population dynamics [9]. Similarly, distributed delays have been employed in epidemic models to account for delayed immune responses, improving the predictive accuracy of disease spread [10].

This paper aims to investigate the dynamic properties of logistic differential equations with distributed delays. Specifically, we analyze the stability, bifurcation, and chaotic dynamics of models incorporating α -distributed delays. By employing the linear chain trick, we convert these models into systems of ordinary differential equations, facilitating both theoretical and numerical analyses.

The paper is structured as follows: we discussed the model of Logistic equation with distributed delay in Section (2). Section (3) presents a stability analysis of continuous-time distributed delay models. In Section (4), we discretize the system and examine its stability properties. Section (5) provides numerical simulations to validate the theoretical findings. Finally, Section (6) concludes with a summary and discussion of future research directions.

2. Model Description

The distributed delay logistic differential equation is given by (1.5) is studied in [11, 12, 13, 14]. In this paper, rather than focusing on the discrete delay in equation (1.2), we examine the Logistic equation with an α distributed delay in the form as

$$\frac{dx(t)}{dt} = \rho x(t) - \rho \left(\int_0^t G(t-s) x(s) ds \right)^2. \quad (2.1)$$

This type of logistic model involves differential equations with distributed delays but differs significantly in how the delayed terms are represented. In equation (2.1), the delay term incorporates the square of the integral of past states $x(t)$, weighted by a kernel function $G(t)$. This structure suggests that the influence of past states accumulates over time and is subsequently squared, which can result in a nonlinear amplification of historical effects on the current state.

We take the kernel function as the weak kernel [15, 16], The exponential kernel models a fading memory effect, where past states influence the present state with a gradually decreasing weight. This is biologically and physically realistic in many applications, such as population dynamics and neural networks.

The exponential kernel allows the linear chain trick (or reduction method) to transform a delay differential equation (DDE) into a system of ordinary differential equations (ODEs). This transformation simplifies numerical simulations and theoretical analysis.

$$G(t) = e^{-\alpha t}, \quad \alpha > 0,$$

then, (1.6) can be written as:

$$\frac{dx(t)}{dt} = \rho x(t) - \rho \left(\int_0^t e^{-\alpha(t-s)} x(s) ds \right)^2, \quad (2.2)$$

$$x(0) = x_0.$$

By applying the linear chain trick [7, 11], these types of Logistic with distributed delay are converted into systems of ordinary differential equations, making them more straightforward to analyze and solve.

we assume that

$$y(t) = \int_0^t e^{-\alpha(t-s)} x(s) ds,$$

$$\frac{dy(t)}{dt} = x - \alpha y.$$

then we obtain feedback control of the α – distributed delay Logistic differential equations corresponding to problem (2.2) as the following system:

$$\begin{aligned} \frac{dx(t)}{dt} &= \rho(x(t) - y^2(t)), & x(0) &= x_0, \\ \frac{dy(t)}{dt} &= x - \alpha y(t), & y(0) &= 0. \end{aligned} \quad (2.3)$$

3. The Continuous Time Model of (2.3)

3.1. The fixed points and Stability analysis of model (2.3)

Stability analysis aims to determine under what conditions the solutions of the Logistic equation converge or diverge. Stability criteria involve examining the eigenvalues of the associated characteristic equation, which is derived from linearizing the system around its equilibrium points.

Here, we study the local stability of (2.3). First, we solve the following equations to find the equilibrium points

$$\begin{aligned} \rho(x - y^2) &= 0, \\ x - \alpha y &= 0. \end{aligned}$$

we get the equilibrium points $(0, 0)$ and (α^2, α) . Now, we linearize (2.3) at the equilibrium point and the Jacobian matrix of the system is given by

$$J = \begin{bmatrix} \rho & -2\rho y^* \\ 1 & -\alpha \end{bmatrix} \quad (3.1)$$

The corresponding characteristic polynomial has trace $T = \rho - \alpha$ and a determinant $D = -\alpha\rho + 2\rho y^*$. The eigenvalues of the Jacobian matrix are

$$\lambda_{1,2} = \frac{1}{2}(T \pm \sqrt{\Delta}),$$

where $\Delta = T^2 - 4D$, $T = \text{trace}(J)$ and $D = \det(J)$.

The trace-determined method [17, 18] offers a simple yet powerful tool for analyzing the stability of continuous time system using the lemma (3.1).

The trace-determined method [17, 18] offers a simple yet powerful tool for analyzing the stability of continuous time system using the lemma (3.1).

Lemma 3.1. The fixed points (x^*, y^*)

- (1) If $\Delta > 0$, $D > 0$ and $\tau < 0$ the fixed point is stable node.
- (2) If $\Delta > 0$, $D > 0$ and $\tau > 0$ the fixed point is unstable node.
- (3) If $\Delta < 0$, $D > 0$ and $\tau < 0$ the fixed point is stable spiral.
- (4) If $\Delta < 0$, $D > 0$ and $\tau > 0$ the fixed point is unstable spiral.

Proposition 3.2. Stability of the system (2.3)

- (1) If $\rho < \alpha$ and $\rho^2 + \alpha^2 < 6\rho\alpha$ the eigenvalues for the first equilibrium point are complex conjugates with negative real parts, indicating it is a stable spiral (stable focus).
- (2) If $\rho > \alpha$ and $\rho^2 + \alpha^2 < 6\rho\alpha$ the eigenvalues for the first equilibrium point are negative real indicating, it is an unstable spiral.
- (3) If $\rho < \alpha$ and $\rho^2 + \alpha^2 > 6\rho\alpha$ the eigenvalues for the first equilibrium point are negative real indicating, it is a stable node.
- (4) If $\rho > \alpha$ and $\rho^2 + \alpha^2 > 6\rho\alpha$, then it is a unstable node.
- (5) If $\rho = \alpha$ and $\rho^2 + \alpha^2 < 6\rho\alpha$, then it is a center node.
- (6) The fixed point $(0, 0)$ is an unstable saddle node.

In Figure 1 shows that the stability region typically shows the behavior of a dynamical system near equilibrium points. In this graph, the stability region is represented by the area where trajectories of the system converge towards an equilibrium point, often indicating a stable node in green or a stable spiral in blue color. Outside this stability region, the system behaves differently, possibly moving away from equilibrium, indicating instability.

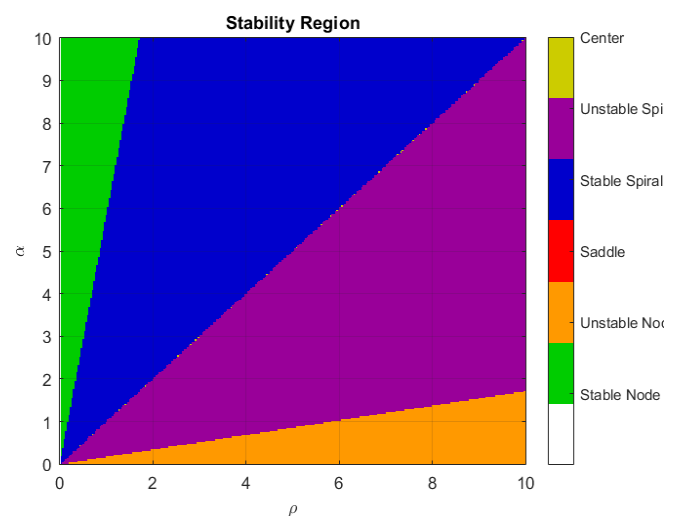


Figure 1. Stability regions for System (2.3).

4. Discrete-time version of (2.3)

4.1. Stability of discretized system

Now, we use piecewise constant arguments method [11, 19, 20] to discretize the system (2.3) as follows:

$$\begin{aligned} x_{n+1} &= x_n + r\rho(x_n - y_n), \quad x(0) = x_0, \\ y_{n+1} &= y_n + r(x_n - \alpha y_n), \quad y(0) = 0. \end{aligned} \quad (4.1)$$

Now, we study the local stability of the fixed points of discretized system (4.1). The Jacobian matrix of the system (4.1) is given by

$$J(x^*, y^*) = \begin{bmatrix} 1 + r\rho & -2r\rho y^* \\ r & 1 - \alpha r \end{bmatrix}. \quad (4.2)$$

The characteristic equation of the Jacobian matrix at the positive fixed point can be written as

$$F(\lambda) = |J - \lambda I| = \lambda^2 + P\lambda + Q = 0, \quad (4.3)$$

where

$$P = (\alpha - \rho)r - 2,$$

and

$$Q = 1 - r(\alpha - \rho) + r^2\rho\alpha.$$

In order to study the modulus of eigenvalues of the characteristic equation (local stability),

We first know the following lemma (4.1), which is the relations between roots and coefficients of the quadratic equation.

Lemma 4.1. [21, 22] *let $F(\lambda) = \lambda^2 + P\lambda + Q = 0$. Suppose that $F(1) > 0$, $\lambda_{1,2}$ are two roots of $F(\lambda) = 0$, then*

- $|\lambda_1| < 1$ and $|\lambda_2| < 1$ if and only if $F(-1) > 0$ and $Q < 1$.
- $|\lambda_1| > 1$ and $|\lambda_2| < 1$ or $(|\lambda_1| < 1$ and $|\lambda_2| > 1)$ if and only if $F(-1) < 0$.
- $|\lambda_1| > 1$ and $|\lambda_2| > 1$ if and only if $F(-1) > 0$ and $Q > 1$.
- $\lambda_1 = -1$ and $\lambda_2 \neq 1$ if and only if $F(-1) = 0$ and $P \neq 0, 2$.
- λ_1 and λ_2 are complex and $|\lambda_1| = |\lambda_2| = 1$ if and only if $P^2 - 4Q < 0$ and $Q = 1$.

Proposition 4.2. *The local stability of the fixed point (α^2, α) of the system (4.1)*

- (1) *It is called sink (asymptotically stable) if $\frac{2\alpha r - 4}{r(\alpha r + 2)} < \rho < \frac{\alpha}{\alpha r + 1}$.*
- (2) *It is called source if $\rho > \max\left\{\frac{\alpha}{\alpha r + 1}, \frac{2\alpha r - 4}{r(\alpha r + 2)}\right\}$.*
- (3) *It is called saddle if $\rho < \frac{2\alpha r - 4}{r(\alpha r + 2)}$.*
- (4) *It is called a nonhyperbolic of the one of the conditions holds:*
 - $\alpha > 4\rho$ and $r = \frac{\alpha \pm \sqrt{\alpha^2 - 4\alpha\rho}}{\alpha\rho}$ where, $r \neq \frac{2}{\alpha}, \frac{4}{\alpha}$.
 - $\frac{\alpha^2 + \rho^2}{\alpha\rho} < 6$ and $r = \frac{1}{\rho} - \frac{1}{\alpha}$.

4.2. Chaos control

In this section we discuss the chaos control method [23, 24] for the feedback control (4.1), to stabilize chaotic of an unstable fixed point of the system. Consider the following controlled form of system (4.1):

$$\begin{aligned} x_{n+1} &= x_n + r\rho(x - y_n^2) + u_n, \\ y_{n+1} &= y_n + r(x_n - \alpha y_n). \end{aligned} \quad (4.4)$$

where, $u_n = -k_1(x_n - x^*) - k_2(y_n - y^*)$ which is the control force, the Jacobian matrix of the new feedback control (4.4) is

$$J(x^*, y^*) = \begin{bmatrix} a_{11} - k_1 & a_{12} - k_2 \\ a_{21} & a_{22} \end{bmatrix}, \quad (4.5)$$

where

$$\begin{aligned} a_{11} &= 1 + r\rho, \\ a_{12} &= -2r\rho y, \\ a_{21} &= r, \\ a_{22} &= 1 - \alpha r. \end{aligned}$$

The characteristic equation of the Jacobian is given by

$$\lambda^2 - (a_{11} + a_{22} - k_1)\lambda + a_{22}(a_{11} - k_1) - a_{21}(a_{12} - k_2) = 0. \quad (4.6)$$

we assume that

$$\lambda_1 + \lambda_2 = a_{11} + a_{22} - k_1, \quad (4.7)$$

and

$$\lambda_1 \lambda_2 = a_{22}(a_{11} - k_1) - a_{21}(a_{12} - k_2). \quad (4.8)$$

The equations $\lambda_1 = \pm 1$ and $\lambda_1 \lambda_2 = 1$ must be solved to get the lines of marginal stability. These requirements ensure that the modulus of the eigenvalues λ_1 and λ_2 is smaller than 1.

The three equations as follows: let $\lambda_1 \lambda_2 = 1$

$$l_1: a_{22}k_1 - a_{21}k_2 = a_{11}a_{22} - a_{12}a_{21} - 1. \quad (4.9)$$

let $\lambda_1 = 1$ in (4.1) and (4.8)

$$l_2: (1 - a_{22})k_1 - a_{21}k_2 = a_{11} + a_{22} - 1 - a_{11}a_{22} + a_{12}a_{21}. \quad (4.10)$$

let $\lambda_1 = -1$ in (4.1) and (4.8)

$$l_3: (1 + a_{22})k_1 - a_{21}k_2 = a_{11} + a_{22} + 1 + a_{11}a_{22} - a_{12}a_{21}. \quad (4.11)$$

The stable eigenvalues lie in the triangular region bounded by l_1 , l_2 and l_3 as in numerical simulation.

5. Numerical results

This study investigates the dynamical behavior of (4.1), focusing on its bifurcation diagrams, maximal Lyapunov exponents, and phase portraits. Through numerical simulations, we explore the transitions between stability and chaos, the sensitivity of the system to initial conditions, and the nature of its equilibrium states. We analyze the bifurcation structure and chaotic behavior by varying the bifurcation parameter r and α , while keeping other

parameters fixed. Additionally, the role of the damping parameter α in enhancing stability is examined. We use the initial condition $(x_0, y_0) = (0.1, 0.1)$ and vary the parameter r and α to study the system's behavior.

The bifurcation diagram of system (4.1), as illustrated in (Figures 2a and 2c), highlights crucial changes in the system's dynamics as the bifurcation parameter r varies. As r increases, the system initially exhibits stable behavior but undergoes Neimark-Sacker bifurcations at $r = 0.158$ and $r = 0.3$ for parameters $\rho = 2$ and $\alpha = 3, \alpha = 5$. Neimark-Sacker bifurcations, occurring in discrete-time dynamical systems, mark a shift from stable fixed points or periodic orbits to more intricate and complex dynamics.

In terms of Lyapunov exponents, these bifurcations correspond to changes in the stability of orbits. At the onset of chaos, the maximum Lyapunov exponent becomes positive, indicating sensitive dependence on initial conditions, which is characteristic of chaotic dynamics. In Figure 2b, the first signs of chaos appear at $r = 0.165$, where the bifurcation diagram begins to display aperiodic, dense points instead of discrete or periodic structures, confirming the presence of chaotic behavior. Similarly, in (Figure 2d), chaos emerges at $r = 0.3$.

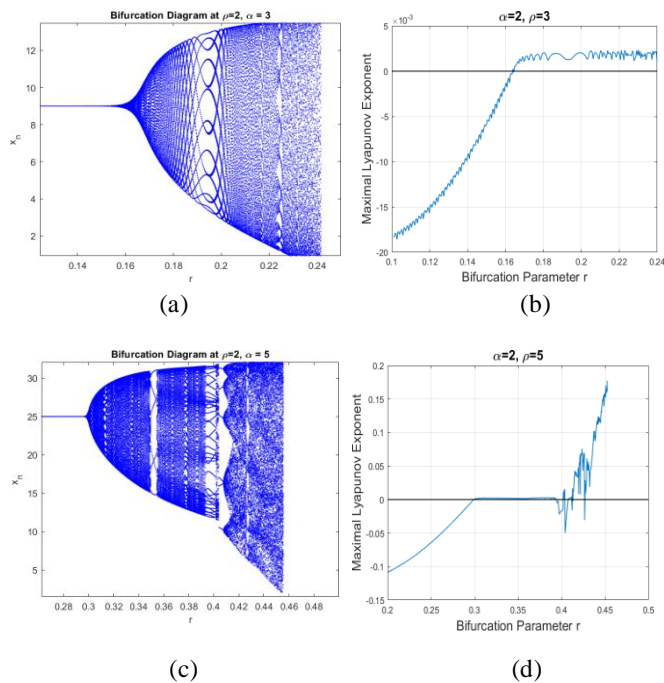


Figure 2. The bifurcation diagrams and maximal Lyapunov exponents with varying r at fixed $\alpha = 3, 5$ and $\rho = 2$.

The bifurcation diagrams for System (4.1) with a fixed bifurcation parameter $r = 0.1$ and varying values of α reveals notable dynamical transitions. Figures 3a and 3c display these bifurcation diagrams for two distinct values of ρ . In Figure 3a, where $\rho = 2$, the system undergoes a

Neimark-Sacker bifurcation at $\alpha = 2.6$. Similarly, in (Figure 3c), with $\rho = 5$, the bifurcation diagram shows that a Neimark-Sacker bifurcation occurs at a higher value of $\alpha = 10.2$.

In our numerical simulations, an interesting observation emerges as the parameter α increases beyond certain thresholds, the bifurcation phenomena begin to diminish, leading to a stabilization of the system's dynamics. Specifically, in both (Figures 3a and 3c), when α is increased significantly above the Neimark-Sacker bifurcation points at $\alpha = 2.6$ for $\rho = 2$ and $\alpha = 10.2$ for $\rho = 5$, the bifurcation behavior is no longer observed. This stabilization suggests that larger values of α suppress the system's tendency towards complex or chaotic dynamics, promoting stability.

This phenomenon indicates that higher α values may strengthen the system's resistance to oscillatory or quasi-periodic behavior that typically arises from bifurcations. Consequently, for sufficiently large α , the system settles into stable fixed points or regular orbits, bypassing chaotic regimes entirely.

To examine the effects of varying r and α on the system's behavior, we present detailed phase portraits and time series for both parameters.

When r varies and $\rho = 2, \alpha = 3$ are fixed, the system's stability significantly changes. When r is increased beyond 0.16, the system becomes more unstable, as shown in the phase portraits and the time series clearly shows the onset of oscillations in the (Figure 4).

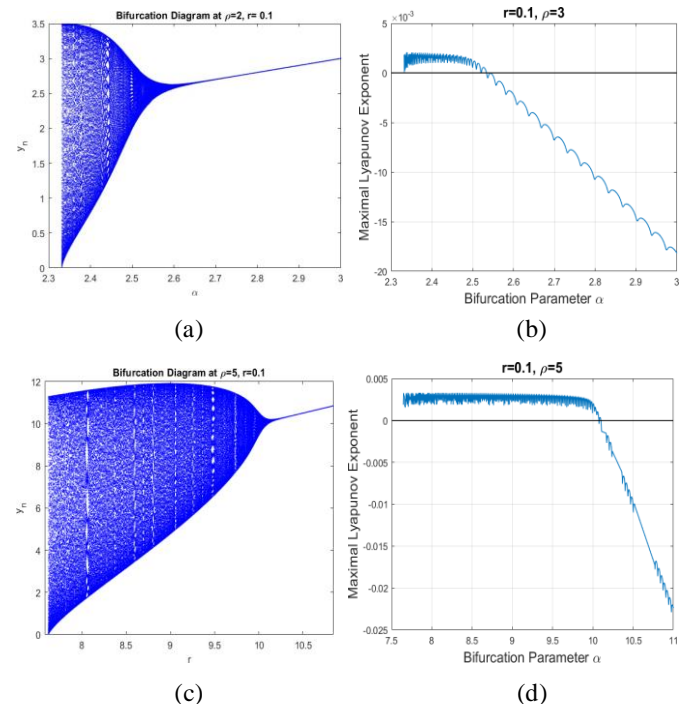


Figure 3. The bifurcation diagrams and maximal Lyapunov exponents with varying α at fixed $r = 0.1$ and $\rho = 2, 5$.

On the other hand, the effect of varies α and $\rho = 5, r = 0.1$ are fixed, the system exhibits periodic but unstable behavior, where the trajectories form closed loops in the phase portrait, but the system does not settle to a stable fixed point as in (Figures 5a and 5b). The system exhibits periodic oscillations, clearly visible in the time series plot. These oscillations persist as the system approaches stability, but as α is increased, the system reaches a stable state more quickly. This is evident in (Figures 5c, 5d and 5e) where higher values of α lead to faster stabilization, reducing the time required for the system to converge to its equilibrium point.

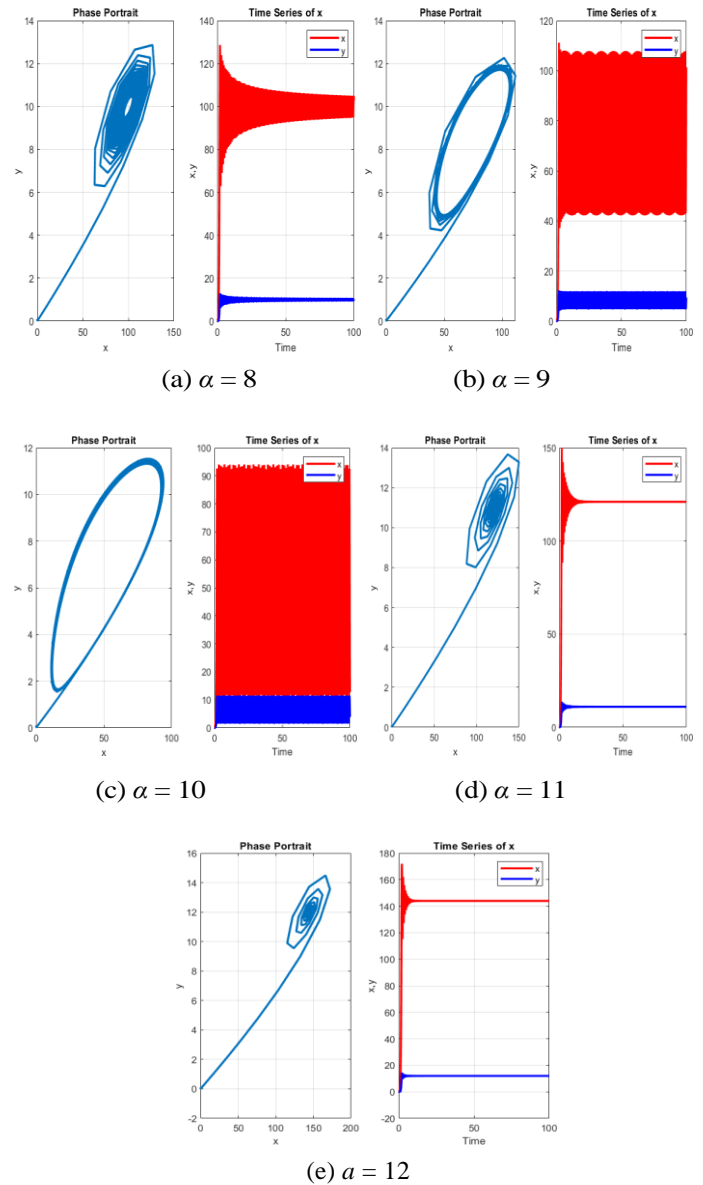


Figure 5. The phase diagrams of the system with varying α and fixed $\rho = 5$ and $r = 0.1$.

To explore how state feedback controls the unstable fixed point in a chaotic system, we performed numerical simulations with the following fixed parameter values: $\alpha = 8, r = 0.1$, and $\rho = 5$. The feedback gains were set to $k_1 = 3$ and $k_2 = 2$, with the initial conditions starting at $(0.1, 0.1)$. This setup was chosen to stabilize the system within a bounded triangular region, leading to a more stable dynamics despite the inherent chaotic behavior of the system as in (Figure 6). The feedback control parameters $k_1 = 3$ and $k_2 = 2$ within this triangular region effectively mitigate the system's sensitivity to initial conditions and promote stability by modifying the response of the system near the fixed point. Chaos control in this context is evident through the application of the feedback mechanism, which

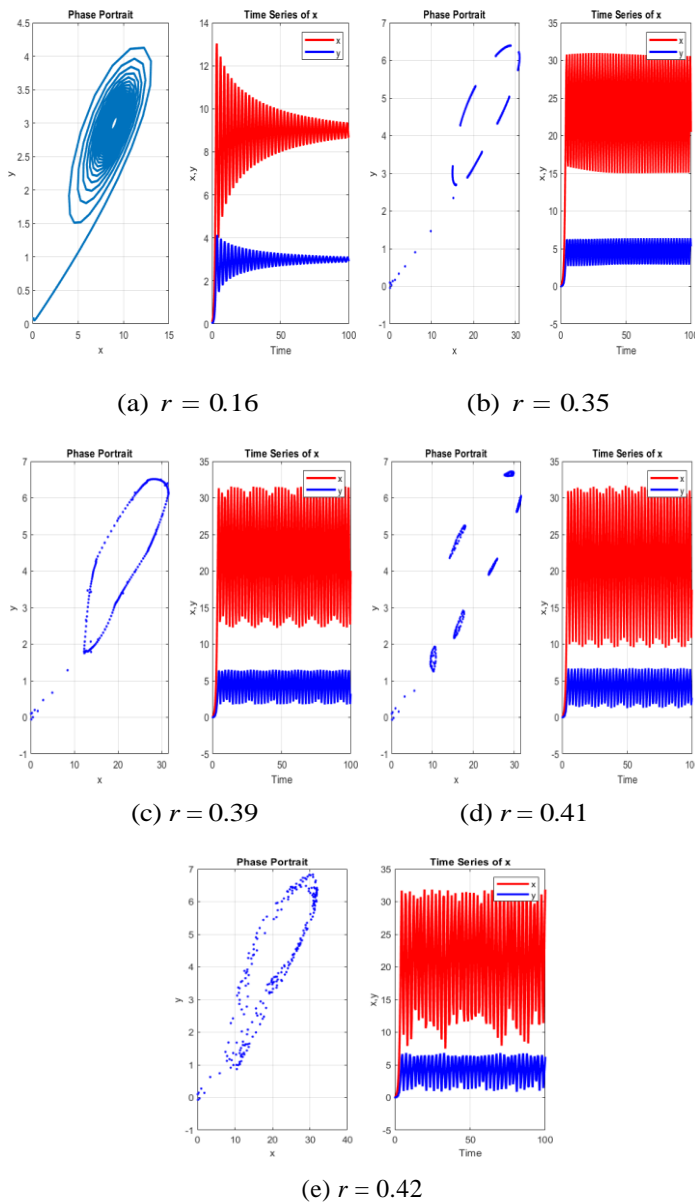


Figure 4. The phase diagrams of the system with varying r and fixed $\rho = 2$ and $\alpha = 3$.

stabilizes the system by steering the trajectory towards the fixed point and preventing the system from exhibiting chaotic oscillations. **Figure 7** shows the time series before and after the chaos control (from iterations 200 to 400) vividly illustrate this transition, where chaotic fluctuations gradually dampen, and the system converges to a stable fixed point.

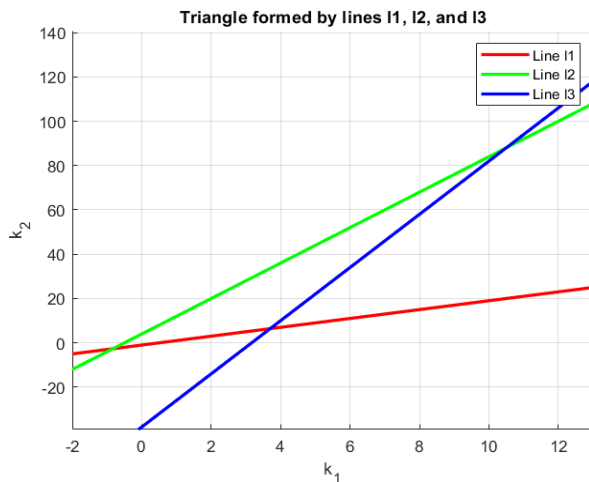
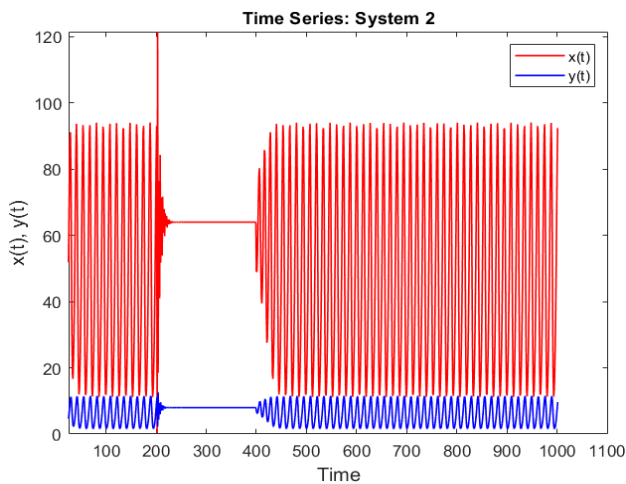


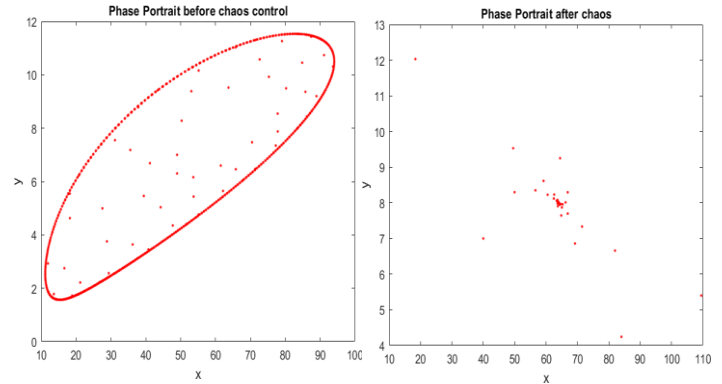
Figure 6. The bounded triangle for the stabilize the fixed point for $\alpha = 8, r = 0.1, \rho = 5$.



a) The time series for x before chaos control

Figure 7. The effect of chaos control parameters at fixing parameters $\alpha = 8, r = 0.1, \rho = 5$.

Furthermore, the phase portraits before and after the chaos control (shown in two separate figures) reinforce the effectiveness of the feedback control. Before applying the control, the phase portraits display a periodic behavior as in (**Figure 8a**). After applying the control, the trajectories in the phase portraits stabilize, indicating the successful suppression of chaotic dynamics and the convergence to a stable equilibrium point as in (**Figure 8b**).



a) The phase portrait before control b) The phase portrait after control

Figure 8. The phase diagram for the controlled system with $\alpha = 3.9, r = 0.4, \rho = 50$, at $k_1 = 1.5, k_2 = -6$.

6. Conclusion

In summary, this research investigates the dynamic behavior of the logistic differential equation with distributed delays in both continuous and discrete time settings. The findings demonstrate that the delay parameter α plays a pivotal role in regulating system stability, with variations in its value driving transitions between stable, periodic, and chaotic behaviors. By employing bifurcation analysis and simulations of maximum Lyapunov exponents, critical shifts in system dynamics are identified, including the emergence of chaos. Furthermore, the study highlights that implementing suitable chaos control strategies can effectively mitigate chaotic behavior, resulting in more predictable and stable outcomes.

The analysis underscores the system's sensitivity to key parameter changes, emphasizing the necessity of precise tuning for practical applications. The bifurcation diagrams and Lyapunov exponent analysis provide valuable insights into stability, enhancing the understanding of how delays and parameter adjustments influence the overall dynamics. These findings hold significant relevance for areas such as biology, population dynamics, and control theory, offering important guidance for designing and managing systems affected by distributed delays in both continuous and discrete-time domains.

In future work, we plan to explore extensions related to our study, including nonlinear and time-dependent delays, the impact of singular perturbations, and the development of advanced chaos control strategies. Additionally, we will discuss potential applications in biological systems.

References

- [1] Tsoularis, A.; Wallace, J. Analysis of logistic growth models. *Math. Biosci.* 2002, 179 (1), 21–55.
- [2] Masani, P.R. Norbert Wiener 1894–1964; Birkhäuser: Basel, 2012; Vol. 5.
- [3] Arino, J.; Wang, L.; Wolkowicz, G.S.K. An alternative formulation for a delayed logistic equation. *J. Theor. Biol.* 2006, 241 (1), 109–119.

- [4] Ruan, S. Delay differential equations in single species dynamics. In *Delay Differential Equations and Applications*; Springer: New York, 2006; pp. 477–517.
- [5] Cooke, K.L.; Grossman, Z. Discrete delay, distributed delay and stability switches. *J. Math. Anal. Appl.* 1982, 86 (2), 592–607.
- [6] Huang, C.; Vandewalle, S. An analysis of delay-dependent stability for ordinary and partial differential equations with fixed and distributed delays. *SIAM J. Sci. Comput.* 2004, 25 (5), 1608–1632.
- [7] Smith, H.L. *An Introduction to Delay Differential Equations with Applications to the Life Sciences*; Springer: New York, 2011; Vol. 57.
- [8] Yuan, Y.; Bélair, J. Stability and Hopf bifurcation analysis for functional differential equation with distributed delay. *SIAM J. Appl. Dyn. Syst.* 2011, 10 (2), 551–581.
- [9] Zhang, C.-H.; Yan, X.-P.; Cui, G.-H. Hopf bifurcations in a predator–prey system with a discrete delay and a distributed delay. *Nonlinear Anal.: Real World Appl.* 2010, 11 (5), 4141–4153.
- [10] Bajiyya, V.P.; Tripathi, J.P.; Kakkar, V.; Wang, J.; Sun, G. Global dynamics of a multi-group SEIR epidemic model with infection age. *Chin. Ann. Math., Ser. B* 2021, 42 (6), 833–860.
- [11] El-Sayed, A.M.A.; Salman, S.M.; Saad, M.A. On some dynamic properties of a distributed delay model. *Bull. Math. Anal. Appl.* 2024, 16 (4), 1821–1291.
- [12] El-Sayed, A.M.A.; Salman, S.M.; Saad, M.A. On the dynamic properties of a distributed delay model. *Appl. Anal. Optim.* 2024, 8 (3), 355–370.
- [13] Lin, C.-J.; Wang, L.; Wolkowicz, G.S.K. An alternative formulation for a distributed delayed logistic equation. *Bull. Math. Biol.* 2018, 80, 1713–1735.
- [14] Rasmussen, H.; Wake, G.C.; Donaldson, J. Analysis of a class of distributed delay logistic differential equations. *Math. Comput. Model.* 2003, 38 (1-2), 123–132.
- [15] Shi, X.; Zhou, X.; Song, X. Dynamical behavior for an eco-epidemiological model with discrete and distributed delay. *J. Appl. Math. Comput.* 2010, 33 (1-2), 305–325.
- [16] Wu, J.; Zhan, X.-S.; Zhang, X.-H.; Gao, H.-L. Stability and Hopf bifurcation analysis on a numerical discretization of the distributed delay equation. *Chin. Phys. Lett.* 2012, 29 (5), 050203.
- [17] Hirsch, M.W.; Smale, S.; Devaney, R.L. *Differential equations, dynamical systems, and an introduction to chaos*; Academic Press: Cambridge, MA, 2012.
- [18] Lathrop, D. *Nonlinear Dynamics and Chaos: With Applications to Physics, Biology, Chemistry, and Engineering*; American Institute of Physics: College Park, MD, 2015.
- [19] Akhmet, M.U. Stability of differential equations with piecewise constant arguments of generalized type. *Nonlinear Analysis: Theory, Methods & Applications* 2008, 68 (4), 794–803.
- [20] El-Sayed, A.M.A.; Salman, S.M. Chaos and bifurcation of the logistic discontinuous dynamical systems with piecewise constant arguments. *Malaya J. Matematik* 2013, 1 (3), 14–20.
- [21] He, Z.; Lai, X. Bifurcation and chaotic behavior of a discrete-time predator–prey system. *Nonlinear Anal.: Real World Appl.* 2011, 12 (1), 403–417.
- [22] Kuznetsov, Y.A. *Elements of applied bifurcation theory*; Springer: Berlin, 1998; Vol. 112.
- [23] Chen, G.; Dong, X. *From chaos to order: methodologies, perspectives and applications*; World Scientific: Singapore, 1998; Vol. 24.
- [24] Lynch, S. *Dynamical Systems with Applications Using Mathematica*; Springer: New York, 2007.